Research Square

Preprints are preliminary reports that have not undergone peer review.
They should not be considered conclusive, used to inform clinical practice,
or referenced by the media as validated information.

PMAIP1 is associated with thyroid carcinoma progression and co-occurs with the activation of ER stress and EMT- related signaling

Jing Wu
Inner Mongolia Autonomous Region People's Hospital
Qiang Song
Baotou Central Hospital
Yizeng Wang
Tianjin Medical University General Hospital
Junyue Li
Tianjin Medical University General Hospital
Dongdong Duan
Inner Mongolia Autonomous Region People's Hospital
Jifan Wang
Inner Mongolia Autonomous Region People's Hospital
Xinyu Ma
Inner Mongolia Autonomous Region People's Hospital
Gang Xue
Baotou Medical College
Xiaobiao Song
Baotou Central Hospital
Bo Zhang
954566556@qq.com

Inner Mongolia Autonomous Region People's Hospital

Research Article

Keywords: papillary thyroid carcinoma, PMAIP1, ER stress, PERK-CHOP, epithelial-mesenchymal transition, single-cell RNA sequencing

Posted Date: October 21st, 2026

DOI: https://doi.org/10.21203/rs.3.rs-11174517/v1

License: This work is licensed under a Creative Commons Attribution 4.0 International License.
Read Full License

Additional Declarations: No competing interests reported.

Abstract

Endoplasmic reticulum (ER) stress is associated with the progression of thyroid cancer (TC). We identified an ER stress-related gene, PMAIP1, and studied its expression and function in TC. We integrated bulk RNA sequencing data and single-cell RNA sequencing data from the thyroid carcinoma (THCA) cohort of The Cancer Genome Atlas (TCGA). Through differential expression analysis, univariate and multivariate Cox regression analysis, and Kaplan–Meier analysis, we found that the ER stress-related gene PMAIP1 is associated with TC prognosis. Higher expression of PMAIP1 is associated with advanced clinical stage and lymph node metastasis. Single-cell analysis showed that PMAIP1 is mainly expressed in malignant thyroid epithelial cells and enriched in metastatic lesions. In TC cells, overexpression of PMAIP1 enhanced the proliferation, colony formation, migration, and invasion of TPC-1 cells as assessed by CCK-8, colony formation, Transwell migration/invasion, and Western blot assays, whereas shRNA-mediated knockdown of PMAIP1 produced the opposite effect in CAL-62 cells. The expression of PMAIP1 is associated with the activation of the PERK-CHOP pathway and changes related to epithelial mesenchymal transition (EMT). Overall, the upregulation of PMAIP1 is associated with thyroid cancer progression, metastatic potential, and invasive cell phenotype, and warrants further mechanistic research and clinical validation.

Introduction

Thyroid cancer is the most common endocrine malignancy, and its global incidence has risen markedly over the past several decades[1]. Papillary thyroid carcinoma (PTC) accounts for the majority of thyroid cancers and generally follows an indolent course with favorable long-term survival[2, 3]. However, a considerable proportion of patients still develop extrathyroidal extension, lymph node or distant metastasis, radioactive iodine-refractory disease, or recurrence, all of which are associated with poorer prognosis[2]. Endoplasmic reticulum (ER) stress-related signaling is important in cancer initiation, progression, and treatment resistance. The unfolded protein response is regulated by three endoplasmic reticulum-resident sensors, which are PERK, IRE1α, and ATF6[4–7]. They restore proteostasis under acute stress, but can trigger apoptosis if stress is severe or sustained. In cancer, the output of the unfolded protein response is context-dependent: transient or low-level unfolded protein response activation is associated with adaptation, survival, angiogenesis, metabolic reprogramming, and metastatic capacity; strong or sustained signaling can promote cell death through CHOP[4–7]. In particular, the PERK-eIF2α-ATF4-CHOP axis has been closely associated with epithelial-mesenchymal transition, invasion, and metastasis in multiple solid tumors, such as thyroid cancer[8–10]. In thyroid cancer, ER stress markers such as GRP78 have been found to correlate with aggressive features[11]. Recent functional studies further link EMT-associated signaling to PTC proliferation and metastatic behavior[12]. Nevertheless, many specific endoplasmic reticulum stress-related genes associated with PTC have not been fully elucidated.

PMAIP1 encodes NOXA. NOXA is a pro-apoptotic member of the BCL-2 family[13, 14]. Under genotoxic stress, it is a direct transcriptional target of ATF4/CHOP downstream of PERK signaling as well as of

p53[13, 15]. It is a canonical apoptosis effector, and it is expected to inhibit tumor growth. Although it exhibits tumor-suppressive roles in certain malignancies such as gastric and triple-negative breast cancers[16, 17], emerging evidence indicates that PMAIP1 is associated with poor prognosis and tumor progression in other solid tumors, including lung adenocarcinoma and colorectal cancer [18, 19]. These contradictory observations suggest that PMAIP1's function may be related to tumor type and microenvironment, which raises questions about whether or how it participates in the pathogenesis of PTC[16–20]. To the best of our knowledge, there is no systematic study on PMAIP1 expression patterns, clinical relevance and biological function in PTC.

Single-cell RNA sequencing (scRNA-seq) can resolve intratumoral heterogeneity, and can also explore the malignant cell state between matched primary lesions and metastatic lesions[21, 22]. In PTC research, such methods can help clarify the expression of candidate genes in malignant thyroid cell or stromal/immune compartments, and also explain the changes in metastatic axis expression[23]. In this study, we hypothesized that specific ER stress-related genes are associated with PTC progression and aggressive phenotypes. To test this hypothesis, we integrated bulk RNA-seq data from TCGA-THCA[3] with single-cell RNA-seq data from GSE184362[21], which included matched primary, lymph node, and subcutaneous metastatic lesions, and performed in vitro gain-of-function and loss-of-function experiments in TPC-1 and CAL-62 cell lines. Our findings indicate that PMAIP1 is an ER stress-related gene closely associated with poor overall survival; its expression changes in parallel with advanced clinicopathological features and metastatic enrichment in malignant thyroid cells at single-cell resolution; and PMAIP1 modulation is closely associated with coordinated changes in proliferation, migration, invasion, and EMT markers, together with activation of the PERK-CHOP pathway.

Materials and Methods

Data sources and preprocessing

Gene-expression count data, FPKM data, and the corresponding clinical annotation files for thyroid carcinoma (THCA) were downloaded from the UCSC Xena platform (https://xenabrowser.net/). Samples were classified according to positions 14–15 of the sample barcode: “01” denoted tumor tissue, whereas “11” denoted adjacent normal tissue. Endoplasmic reticulum stress–related genes were collected from the GeneCards database and relevant publications. After duplicate entries were removed, the resulting gene set was saved as ER_stress_genes.csv (Supplementary Data 1).

Differential expression analysis of endoplasmic reticulum stress–related genes

Genes shared by the expression matrix and the endoplasmic reticulum stress gene set were extracted for further analysis. For each gene, differential expression between tumor and adjacent normal tissues was evaluated. The $\log_2$ fold change ($\log_2$FC) was calculated, and P values were adjusted using the

Benjamini–Hochberg procedure to obtain false discovery rates (FDRs). Genes with an absolute $\log_2$FC greater than 1 and an FDR below 0.05 were considered differentially expressed. A volcano plot was generated with the ggplot2 and ggrepel packages, with the five most strongly upregulated and five most strongly downregulated genes labeled.

Identification of prognostic genes and survival analysis

The FPKM expression matrix was integrated with overall survival (OS) data and survival-status information. Univariate Cox proportional hazards regression was performed separately for every endoplasmic reticulum stress–related gene included in the differential expression analysis. Hazard ratios (HRs) and corresponding 95% confidence intervals (CIs) were calculated. PMAIP1, which showed the largest HR, was selected for subsequent analyses.

The surv_cutpoint function was used to determine the optimal PMAIP1 expression threshold. Patients were then divided into high- and low-expression groups according to this cutoff. Kaplan–Meier survival curves were generated, and differences between groups were assessed using the log-rank test. In addition, bidirectional stepwise variable selection was applied to construct a multivariable Cox proportional hazards model, thereby evaluating whether PMAIP1 was an independent prognostic factor.

Gene set enrichment analysis

TCGA-THCA samples were stratified into high- and low-PMAIP1-expression groups according to the median PMAIP1 expression level. For every gene, the $\log_2$ fold change between the two groups was calculated, and the genes were ranked in descending order. This pre-ranked gene list was analyzed with the clusterProfiler and GSEABase packages. Gene set enrichment analysis was performed using the Hallmark collection from MSigDB (h.all.v2024.1), the KEGG collection (c2.cp.kegg.v7.4), and Gene Ontology biological-process gene sets.

Pathways with an adjusted P value (false discovery rate, FDR < 0.05) were regarded as significantly enriched. Individual enrichment curves were produced with the GseaVis package, while a multi-pathway enrichment bubble plot was generated using ggplot2.

Association between PMAIP1 expression and clinicopathological characteristics

Clinical records were reviewed to obtain T, N, and M classifications, together with the overall clinical stage. Substages were consolidated where appropriate; for example, T1a and T1b were combined into T1, and stages IVA–IVC were grouped as stage IV. Samples with missing staging information were excluded.

PMAIP1 FPKM values were compared across the different clinical stages. The Wilcoxon rank-sum test was used for comparisons involving two groups, whereas the Kruskal–Wallis test was used for comparisons involving more than two groups. Box plots or violin plots overlaid with individual data points were prepared with ggpubr and ggplot2, and the corresponding significance P values were displayed.

Single-cell RNA sequencing analysis

The thyroid cancer single-cell RNA-sequencing dataset GSE184362 was downloaded from the Gene Expression Omnibus (GEO). This dataset included primary tumor (PT), lymph-node metastasis (LN), and subcutaneous metastasis (SubQ) samples.

Downstream processing was conducted with Seurat version 5. Cells expressing 200–5,000 genes were retained, together with cells containing more than 1,000 total UMIs, a mitochondrial gene fraction of no more than 10%, and an erythrocyte-associated gene fraction of no more than 10%. The data were normalized using LogNormalize. Highly variable genes were identified with FindVariableFeatures, followed by scaling with ScaleData and principal-component analysis using RunPCA. Harmony was utilized to correct for batch effects. The integrated data were visualized via t-SNE, and graph-based clustering was performed at a resolution of 0.3.

Cell clusters were annotated according to canonical marker genes: thyroid epithelial cells (TG, EPCAM), T/NK cells (CD3D, CD3E), B/plasma cells (MS4A1, CD79A), myeloid cells (CD14, LYZ), fibroblasts (COL1A1, DCN), endothelial cells (VWF, CD34), and pericytes (RGS5, ACTA2). The expression distribution of PMAIP1 across the annotated cell populations was then examined. Thyroid epithelial cells were stratified by sample origin (PT, LN, and SubQ), and PMAIP1 expression was compared among these groups. To distinguish malignant from benign epithelial cells, copy number variations were inferred using inferCNV with T/NK cells and fibroblasts as normal reference populations, and CopyKAT was applied to predict aneuploid cells; epithelial cells supported by concordant copy-number evidence from both approaches were defined as malignant thyroid epithelial cells.

Cell culture and transfection

Two human thyroid cancer cell lines were employed for the in vitro functional studies: TPC-1 (ATCC #CRL-1451), originating from papillary thyroid carcinoma (PTC), and CAL-62 (CCTCC, Wuhan, China), originating from anaplastic thyroid carcinoma (ATC). Because endogenous PMAIP1 levels are relatively low in TPC-1, this line was chosen for gain-of-function experiments; conversely, the high basal PMAIP1 expression and the highly aggressive, dedifferentiated nature of CAL-62 made this line appropriate for loss-of-function experiments targeting PMAIP1. For overexpression, TPC-1 cells were transfected with a PMAIP1-expression plasmid (OE) or with the corresponding empty vector (Vector); for knockdown, CAL-62 cells were transfected with two PMAIP1-targeting shRNAs (sh1, sh2) or a non-targeting scrambled control (SC). Successful overexpression and knockdown were verified at both the mRNA and protein

levels by qRT-PCR and Western blotting before any downstream assay. STR profiling was used to authenticate both cell lines, and routine mycoplasma testing (most recently in January 2026) remained negative. Only cells within passages 5–15 were used for experiments.

Quantitative real-time PCR (qRT-PCR)

For quantitative real-time PCR (qRT-PCR), total cellular RNA was first isolated with TRIzol reagent and further purified using the RNeasy Mini kit (Vazyme, China). One microgram of total RNA was then subjected to reverse transcription using the PrimeScript RT reagent Kit with gDNA Eraser (Vazyme, China). Amplification reactions were subsequently carried out with Power SYBR Green PCR master mix. Relative expression levels were normalized against GAPDH and calculated by the 2^−ΔΔCt method. The primer sequences used in this study are listed below:

PMAIP1-F: 5'-GCTGGAAGTCGAGTGTGCTA-3'

PMAIP1-R: 5'-GAAACGTGCACCTCCTGAGA-3'

GAPDH-F: 5'-AGCAAGAGCACAAGAGGAAG-3'

GAPDH-R: 5'-GGTTGAGCACAGGGTACTTT-3'

Western blotting analysis

Cells were lysed in RIPA buffer supplemented with protease and phosphatase inhibitors to obtain total protein. The extracted proteins were resolved by SDS-PAGE and electrophoretically transferred onto PVDF membranes, which were then probed overnight at 4°C with the following primary antibodies: anti-PMAIP1 (CST, #14766, WB: 1:1000), anti-CHOP (CST, #2895, WB: 1:1000), anti-PERK (CST, #3192, WB: 1:1000), anti-p-PERK (CST, #3179, WB: 1:1000), anti-E-cadherin (Abcam, ab1416, WB: 1:1000), anti-N-cadherin (Abcam, ab18203, WB: 1:1000), and anti-GAPDH (Santa Cruz Biotechnology, sc-47724, WB: 1:5000), followed by the corresponding secondary antibodies. Immunoreactive bands were detected with a chemiluminescence imaging system. Band intensities from three independent experiments were quantified using ImageJ software. For each sample, the intensity of phosphorylated PERK (p-PERK) was first normalized to that of total PERK, and the resulting value was further normalized to GAPDH as the loading control.

Cell proliferation assay

The CCK-8 assay was applied to evaluate cell proliferation. Cells were seeded into 96-well plates, and the absorbance at 450 nm was recorded on days 0, 1, 2, 3, and 4 after seeding.

Colony formation assay

For the colony formation assay, cells were plated at low density into 6-well plates and maintained in culture for 14 days. The resulting colonies were fixed in 4% paraformaldehyde, stained with 0.1% crystal violet, and counted manually.

Transwell assay

Cell migratory and invasive capacities were examined using Transwell chambers. Invasion assays were performed in chambers pre-coated with Matrigel. Cells suspended in serum-free medium were placed in the upper chamber, whereas the lower chamber received medium supplemented with 20% FBS as a chemoattractant. At 24 h after plating, cells that had traversed the membrane were fixed, stained, and quantified.

Statistical analysis

All bioinformatics analyses were performed in R version 4.4.1. Comparisons between two groups were performed using the Wilcoxon rank-sum test, and comparisons among multiple groups using the Kruskal–Wallis test. Survival differences were evaluated by the log-rank test, and prognostic associations were examined using Cox proportional hazards regression. Gene set enrichment analysis was performed using the pre-ranked GSEA algorithm. For in vitro experiments, data are presented as the mean ± SD of at least three independent experiments, and intergroup comparisons were analyzed using Student's t-test. A two-sided P value < 0.05 or a false discovery rate (FDR) < 0.05 was considered statistically significant.

Results

PMAIP1 is the ER stress-related gene most strongly associated with poor prognosis

To characterize the expression profile of endoplasmic reticulum (ER) stress-related genes in papillary thyroid carcinoma (PTC), we compiled a gene set containing 2,084 ER stress-related genes and examined their expression in the TCGA-THCA cohort. Using $|\log_2 FC| > 1$ and FDR < 0.05 as the criteria, differential expression analysis between tumor tissues and adjacent normal tissues identified 199 significantly upregulated genes (downregulated genes are also indicated in Fig. 1A). The volcano plot showed an overall upregulation pattern of ER stress genes in tumor tissues, with FN1, DCSTAMP, and other genes showing the most pronounced increases, whereas GRIA1, GPC3, UGT2B11, and other genes showed relatively lower expression in tumor tissues (Fig. 1A). To screen for prognostically valuable ER stress genes among the upregulated candidates, we performed univariate Cox regression analysis using overall survival (OS) as the endpoint. This analysis identified a group of genes significantly associated with patient prognosis, including SPP1, PMAIP1, COL26A1, CERS1, and SEZ6L2 (Fig. 1B). Multivariate Cox analysis showed that PMAIP1 had the highest hazard ratio (HR) among all included genes (HR = 1.303, 95% CI: 1.120–1.517, P < 0.001), followed by CERS1 (HR = 1.051, 95% CI: 1.024–1.078, P < 0.001) and SPP1 (HR = 1.005, 95% CI: 1.000-1.010, P = 0.047) (Fig. 1C). Kaplan-Meier survival analysis

confirmed that patients in the PMAIP1-high expression group had significantly shorter overall survival than those in the low-expression group (log-rank P = 0.043; Fig. 1D). GSEA-GO analysis showed that the PMAIP1-high expression group was significantly enriched in the ER stress-induced apoptotic signaling pathway (Fig. 1E). These results suggest that the ER stress pathway may be activated in thyroid cancer. We further examined the expression of key ER stress effector molecules. Western blotting showed that in TPC-1 cells overexpressing PMAIP1, the ER stress marker CHOP was increased and PERK phosphorylation (p-PERK) was markedly enhanced, whereas total PERK protein levels showed no obvious change; in CAL-62 cells with PMAIP1 knockdown, CHOP and p-PERK levels were correspondingly reduced (Fig. 1F). Taken together, these results suggest an association between PMAIP1 expression and activation of the PERK-CHOP-mediated ER stress pathway.

PMAIP1 expression increases with papillary thyroid carcinoma progression

Next, we analyzed the clinicopathological association between PMAIP1 expression and PTC prognosis. PMAIP1 expression was significantly higher in tumor tissues than in adjacent normal tissues (Wilcoxon test, $P = 4.7\times10^{-10}$; Fig. 2A). According to clinical stage, PMAIP1 expression showed an upward trend from stage I to stage IV, with the highest level in stage IV (Kruskal-Wallis test, $P = 3\times10^{-6}$; Fig. 2B). Regarding T stage, PMAIP1 expression was significantly higher in advanced T-stage tumors than in early-stage tumors (Wilcoxon test, $P = 5.5 \times 10^{-6}$; Fig. 2C). The expression level was higher in the lymph node metastasis-positive group than in the lymph node metastasis-negative group (Wilcoxon test, $P = 3.7 \times 10^{-11}$; Fig. 2D). Collectively, these data indicate that PMAIP1 upregulation is associated with clinical features of PTC, including stage, tumor size, and lymph node metastasis status.

Single-cell analyses reveal elevated PMAIP1 in metastatic lesions and its association with malignancy

To determine the cellular origin and tissue distribution of PMAIP1 expression, we analyzed the single-cell RNA sequencing dataset GSE184362, which included paired primary tumor (PT), lymph node metastasis (LN), and subcutaneous metastasis (SubQ) samples. After quality control and data integration, a total of 124,030 cells were retained and annotated into seven major cell populations based on canonical markers: thyroid epithelial cells (TG, EPCAM), T/NK cells (CD3D, CD3E), B/plasma cells (MS4A1, CD79A), myeloid cells (CD14, LYZ), fibroblasts (COL1A1, DCN), endothelial cells (VWF, CD34), and pericytes (RGS5, ACTA2) (Fig. 3A). A dot plot of marker genes showed that the cell populations were well separated (Fig. 3B). Feature plots showed that PMAIP1 was expressed in multiple cell types but was most prominent in the thyroid epithelial cell population (Fig. 3C). Using T/NK cells and fibroblasts as normal references, we applied inferCNV to infer copy number variations and combined this with CopyKAT to predict aneuploid cells. The results showed varying degrees of copy number variation in all three sample types. In the distant metastasis sample, deletions were present on chromosomes 1, 9, 13, and 22, whereas chromosome 7 showed marked amplification; in the lymph node metastasis sample,

chromosomes 1 and 7 were amplified and chromosome 22 was deleted; in the primary tumor sample, marked amplifications were present on chromosomes 1 and 21 (Fig. 3D). After stratifying thyroid epithelial cells by anatomical site, PMAIP1 expression displayed a clear gradient: lowest in the primary tumor, intermediate in the lymph node metastasis, and highest in the subcutaneous (distant) metastasis. Among these malignant thyroid cells, PMAIP1 expression was significantly higher in both lymph node and distant metastases than in the primary tumor (both $P < 2.22 \times 10^{-16}$; Fig. 3E). These single-cell results indicate that PMAIP1 upregulation is prominent in malignant thyroid epithelial cells and becomes further enriched during metastatic progression.

PMAIP1 promotes malignant phenotypes and EMT in thyroid cancer cells

To clarify the functional role of PMAIP1 in thyroid cancer progression, we established gain-of-function and loss-of-function models using TPC-1 cells (derived from PTC) and CAL-62 cells (derived from ATC), respectively. First, stable transfection was used to successfully overexpress PMAIP1 (OE) in TPC-1 cells and knock down PMAIP1 (KD) in CAL-62 cells, with efficiency verified at both the protein and mRNA levels (Fig. 4A). CCK-8 proliferation assays showed that PMAIP1-overexpressing TPC-1 cells exhibited enhanced proliferative capacity in vitro; conversely, proliferation was suppressed in CAL-62 cells with stable PMAIP1 knockdown, and both sh1 and sh2 showed stable inhibitory effects (both $P < 0.001$; Fig. 4B). Colony formation assays further confirmed these findings: TPC-1 cells in the PMAIP1 overexpression group formed significantly more colonies than control cells, whereas CAL-62 cells in the PMAIP1 knockdown group formed markedly fewer colonies with smaller colony sizes (all $P < 0.001$; Fig. 4C). Transwell migration assays showed that PMAIP1 overexpression significantly enhanced the migration and invasion of TPC-1 cells, with a marked increase in the number of cells traversing the membrane; in contrast, PMAIP1 knockdown significantly reduced the numbers of migrating and invading CAL-62 cells (all $P < 0.001$; Fig. 4D). To investigate the molecular mechanisms underlying the association between PMAIP1 and the malignant biological behavior of PTC, we compared tumors with high versus low PMAIP1 expression in the TCGA-THCA cohort and performed GSEA based on Hallmark, KEGG, and Gene Ontology gene sets. Among the Hallmark pathways, the PMAIP1-high expression group showed significant enrichment of epithelial-mesenchymal transition (EMT), apoptosis, IL-6/JAK/STAT3 signaling, the G2M checkpoint, mTORC1 signaling, angiogenesis, PI3K/AKT/mTOR signaling, glycolysis, and hypoxia (all FDR < 0.05; Fig. 4E). We further assessed the expression of EMT-related markers by Western blotting. In PMAIP1-overexpressing TPC-1 cells, expression of the mesenchymal marker N-cadherin was markedly upregulated, whereas expression of the epithelial marker E-cadherin was downregulated; CAL-62 cells with PMAIP1 knockdown showed the opposite pattern, with decreased N-cadherin and increased E-cadherin (Fig. 4F). This result is consistent with the bulk RNA-seq GSEA finding that the EMT pathway was significantly enriched in the PMAIP1-high expression group.

Discussion

In this study, we analyzed ER stress-related genes in PTC and identified PMAIP1, among 2,084 candidate genes in the TCGA-THCA cohort, as the gene most strongly associated with poor overall survival. The PMAIP1 gene encodes the BH3-only protein NOXA and, under ER stress conditions, has traditionally been regarded as a pro-apoptotic effector and a direct transcriptional target of the PERK-eIF2α-ATF4-CHOP signaling axis[13–15]. According to this classical view, PMAIP1 upregulation would be expected to promote apoptosis and thereby exert tumor-suppressive effects; indeed, tumor-suppressive functions have been reported in certain cancer types, such as gastric cancer and triple-negative breast cancer[16, 17]. It is therefore noteworthy that a growing body of evidence indicates that PMAIP1/NOXA is associated with adverse features in multiple solid tumors, including lung adenocarcinoma, colorectal cancer, the quasi-mesenchymal subtype of pancreatic cancer, and, importantly, follicular thyroid carcinoma, in which PMAIP1 is associated with cell proliferation and metastasis through the Wnt3/FOSL1 signaling pathway[18–20]. One plausible explanation for our observations in PTC is that under chronic or low-level ER stress, the unfolded protein response (UPR) can shift from a pro-apoptotic output to adaptive, pro-survival programs[4–7]; in this context, PMAIP1 may be induced as part of a broader PERK-CHOP-coordinated stress response without necessarily causing cell death, particularly when anti-apoptotic buffers such as MCL-1 and BCL-2 remain sufficient[24].

Higher PMAIP1 expression was associated with advanced clinical stage, higher T stage, and lymph node metastasis; single-cell analysis indicated that PMAIP1 was mainly enriched in malignant thyroid epithelial cells, with its expression appearing to increase along the "primary tumor-lymph node-distant metastasis" axis[25].

PMAIP1 expression was mainly confined to malignant thyroid epithelial cells rather than stromal or immune cells; its gradient distribution across primary tumors, lymph node metastases, and subcutaneous metastatic lesions is consistent with clonal selection or adaptive reprogramming during tumor dissemination[21, 26]. From a translational medicine perspective, PMAIP1 may warrant evaluation as a candidate risk-stratification biomarker in papillary thyroid carcinoma (PTC). Although most PTCs follow an indolent course, a subset of patients progress to locoregional or distant metastasis, and biomarkers that can help identify such patients are therefore still needed[27]. The association between PMAIP1 and the PERK-CHOP pathway also raises a hypothetical possibility: tumors with high PMAIP1 expression may exhibit differential sensitivity to UPR-targeted agents or rational combination therapies, for example, PERK pathway inhibitors combined with BH3 mimetics that neutralize MCL-1, an approach that has been explored in hematologic malignancies and other solid tumors[28, 29].

Functional experiments in TPC-1 and CAL-62 cells further showed that PMAIP1 modulation was closely associated with coordinated changes in cell proliferation, colony-forming ability, migration, and invasion, while also involving changes in the PERK-CHOP branch of the UPR pathway and EMT-related molecular features. Overall, these findings suggest that PMAIP1 upregulation may be associated with an aggressive thyroid cancer phenotype, and this association may be mediated through crosstalk between ER stress and EMT-related signaling pathways[8].

Notably, our loss-of-function experiments were performed in CAL-62 cells, which are derived from anaplastic thyroid carcinoma, the most aggressive and dedifferentiated form of thyroid cancer. The observation that PMAIP1 depletion suppressed proliferation, colony formation, migration, and invasion in this highly malignant context suggests that the role of PMAIP1 may extend beyond PTC to dedifferentiated thyroid cancer—a transition that is clinically relevant because a subset of PTCs progressively dedifferentiate toward the anaplastic phenotype[30, 31].

In our data, the co-occurrence of PERK-CHOP activation and EMT-related changes is particularly noteworthy for its mechanistic implications. In TPC-1 cells overexpressing PMAIP1, we observed increased CHOP and p-PERK levels (with no change in total PERK), accompanied by upregulation of N-cadherin and downregulation of E-cadherin; PMAIP1 knockdown in CAL-62 cells produced the opposite pattern. These findings were also supported at the pathway level in TCGA-THCA: GSEA showed that tumors with high PMAIP1 expression were enriched not only for ER stress-induced apoptotic signaling but also for features such as EMT and IL-6/JAK/STAT3 signaling. This combined pattern is consistent with multiple reports indicating that the PERK-eIF2α pathway tends to participate in the regulation of mesenchymal-like tumor cells and can support their invasion and metastasis[8–10]; it is also consistent with previous studies in thyroid cancer showing that ER stress effectors such as GRP78 are associated with metastatic behavior, whereas XBP1s can suppress EMT in PTC[11, 32]. The co-enrichment of EMT with hypoxia, metabolic, and secretory programs in the present study supports a PERK-driven adaptive mesenchymal/secretory state. Therefore, it is reasonable to speculate that as progressive PTC cells encounter microenvironmental stresses such as hypoxia, nutrient limitation, or secretory burden, the PERK-ATF4-CHOP pathway becomes activated and induces PMAIP1, a known CHOP/ATF4 target, together with broader transcriptomic changes related to EMT and tissue remodeling[33, 34]. The increase in p-PERK and CHOP upon PMAIP1 overexpression may reflect a compensatory or feed-forward stress response within the UPR network, although this possibility requires direct mechanistic testing.

This study has several limitations. First, loss-of-function experiments were performed in CAL-62, an anaplastic thyroid carcinoma cell line rather than a PTC-derived line; although this models highly aggressive, dedifferentiated disease, confirmation of these findings in additional PTC-derived cell lines is warranted. Second, PMAIP1 was suppressed by shRNA-mediated knockdown rather than complete knockout, and whether partial suppression phenocopies complete loss remains to be determined. Third, the prognostic analysis was based on the TCGA-THCA cohort, in which the number of death events is limited; accordingly, the optimal expression cutoff defined by the surv_cutpoint function should be regarded as exploratory and requires validation in independent cohorts. Finally, the associations among PMAIP1, PERK-CHOP signaling, and EMT-related changes are correlative; whether PMAIP1 directly drives these pathways or is itself induced as part of a broader stress response remains to be established. Overall, our integrated bulk, single-cell, and functional analyses link PMAIP1 upregulation to thyroid cancer progression and aggressive cellular phenotypes, potentially through crosstalk between PERK–CHOP ER stress signaling and EMT-related pathways.

Conclusions

In summary, this study found that PMAIP1, a gene within an endoplasmic reticulum stress-related gene set, is strongly associated with poor prognosis in PTC. PMAIP1 expression increases with advanced clinical stage, higher T stage, and lymph node metastasis, and single-cell analysis localizes its expression predominantly to malignant thyroid epithelial cells, with further enrichment along the primary tumor–lymph node–distant metastasis axis. Functional experiments demonstrate that PMAIP1 promotes proliferation, colony formation, migration, and invasion in thyroid cancer cells, accompanied by activation of the PERK–CHOP pathway and epithelial–mesenchymal transition-related changes. These findings suggest that PMAIP1 may serve as a candidate prognostic biomarker and potential therapeutic target in PTC. Nevertheless, further mechanistic studies and clinical validation are warranted.

Declarations

Ethics approval and consent to participate

Not applicable. This study did not involve human participants, human tissues, or animals. All analyses were based on publicly available, de-identified datasets (TCGA-THCA and GSE184362), and in vitro experiments were performed using established human cell lines; therefore, ethical approval and informed consent to participate were not required.

Consent for publication

Not applicable. This study does not include any individual person's data in any form (including images, videos, or clinical details); all datasets used are publicly available and de-identified, and therefore consent for publication was not required.

Competing interests

The authors declare no competing interests.

Funding

This work was supported by the Science and Technology Program of the Joint Fund of Scientific Research for the Public Hospitals of Inner Mongolia Academy of Medical Sciences (Grant No. 2024GLLH0112), the National Key Clinical Specialty Development Project (General Surgery), Baotou Central Hospital and the Inner Mongolia Autonomous Region Science and Technology Innovation Guidance Project (Grant No. CXYD 2020BT09).

Author Contribution

Jing Wu, Yizeng Wang, and Qiang Song contributed equally to this work. Jing Wu and Yizeng Wang designed the study, performed the experiments, analyzed the data, and drafted the manuscript. Qiang

Song conducted statistical analysis, and prepared all figures. Junyue Li, Dongdong Duan, and Jifan Wang assisted with data curation. Xinyu Ma and Gang Xue participated in manuscript editing. Bo Zhang and Xiaobiao Song conceived and supervised the study, provided funding support, and critically revised the manuscript. All authors reviewed and approved the final manuscript.

Acknowledgements

We thank The Cancer Genome Atlas (TCGA) initiative, all tissue donors, and the investigators who contributed to acquiring and analyzing the samples used in this study. We also gratefully acknowledge Professor Yu-Long Wang for providing the GSE184362 dataset used in this study, which is available in the GEO database.

Data Availability

The bulk RNA-sequencing expression data and clinical information analyzed in this study were obtained from the TCGA Thyroid Carcinoma cohort (TCGA-THCA) via the UCSC Xena platform (https://xenabrowser.net/datapages/?cohort=GDC%20TCGA%20Thyroid%20Cancer%20(THCA)). The single-cell RNA-sequencing dataset is available in the Gene Expression Omnibus under accession number GSE184362 (https://www.ncbi.nlm.nih.gov/geo/query/acc.cgi?acc=GSE184362). The endoplasmic reticulum stress-related gene set was retrieved from GeneCards (https://www.genecards.org/Search/Keyword?queryString=endoplasmic%20reticulum%20stress) using the keyword "endoplasmic reticulum stress", and the complete gene set is provided as Supplementary Data 1 (ER_stress_genes.csv). The gene-set collections used for GSEA were obtained from the Molecular Signatures Database (MSigDB; https://www.gsea-msigdb.org/gsea/msigdb/human/collections.jsp): the Hallmark collection (h.all.v2024.1), the KEGG curated pathway collection (c2.cp.kegg.v7.4), and Gene Ontology biological-process gene sets.

References

1. Kitahara CM, Schneider AB. Epidemiology of Thyroid Cancer. Cancer Epidemiol Biomarkers Prev. 2022;31:1284–97. https://doi.org/10.1158/1055-9965.EPI-21-1440.
2. Haugen BR, Alexander EK, Bible KC, et al. 2015 American Thyroid Association Management Guidelines for Adult Patients with Thyroid Nodules and Differentiated Thyroid Cancer: The American Thyroid Association Guidelines Task Force on Thyroid Nodules and Differentiated Thyroid Cancer. Thyroid®. 2016;26:1–133. https://doi.org/10.1089/thy.2015.0020.
3. Agrawal N, Akbani R, Aksoy BA, et al. Integrated Genomic Characterization of Papillary Thyroid Carcinoma. Cell. 2014;159:676–90. https://doi.org/10.1016/j.cell.2014.09.050.
4. Walter P, Ron D. The Unfolded Protein Response: From Stress Pathway to Homeostatic Regulation. Science. 2011;334:1081–6. https://doi.org/10.1126/science.1209038.

5. Hetz C. The unfolded protein response: controlling cell fate decisions under ER stress and beyond. Nat Rev Mol Cell Biol. 2012;13:89–102. https://doi.org/10.1038/nrm3270.
6. Wang M, Kaufman RJ. Protein misfolding in the endoplasmic reticulum as a conduit to human disease. Nature. 2016;529:326–35. https://doi.org/10.1038/nature17041.
7. Cubillos-Ruiz JR, Bettigole SE, Glimcher LH. Tumorigenic and Immunosuppressive Effects of Endoplasmic Reticulum Stress in Cancer. Cell. 2017;168:692–706. https://doi.org/10.1016/j.cell.2016.12.004.
8. Feng Y, Sokol ES, Del Vecchio CA, et al. Epithelial-to-Mesenchymal Transition Activates PERK–eIF2α and Sensitizes Cells to Endoplasmic Reticulum Stress. Cancer Discov. 2014;4:702–15. https://doi.org/10.1158/2159-8290.CD-13-0945.
9. Feng Y-X, Jin DX, Sokol ES, et al. Cancer-specific PERK signaling drives invasion and metastasis through CREB3L1. Nat Commun. 2017;8:1079. https://doi.org/10.1038/s41467-017-01052-y.
10. Mujcic H, Nagelkerke A, Rouschop KMA, et al. Hypoxic Activation of the PERK/eIF2α Arm of the Unfolded Protein Response Promotes Metastasis through Induction of LAMP3. Clin Cancer Res. 2013;19:6126–37. https://doi.org/10.1158/1078-0432.CCR-13-0526.
11. Dai Y-J, Qiu Y-B, Jiang R, et al. Concomitant high expression of ERα36, GRP78 and GRP94 is associated with aggressive papillary thyroid cancer behavior. Cell Oncol. 2018;41:269–82. https://doi.org/10.1007/s13402-017-0368-y.
12. Lin B, Jiang X, Bhandari A, et al. FAM20C Promotes Papillary Thyroid Cancer Proliferation and Metastasis via Epithelial–Mesenchymal Transition. Mol Carcinog. 2025;64:152–61. https://doi.org/10.1002/mc.23833.
13. Oda E, Ohki R, Murasawa H, et al. Noxa, a BH3-Only Member of the Bcl-2 Family and Candidate Mediator of p53-Induced Apoptosis. Science. 2000;288:1053–8. https://doi.org/10.1126/science.288.5468.1053.
14. Chen L, Willis SN, Wei A, et al. Differential Targeting of Prosurvival Bcl-2 Proteins by Their BH3-Only Ligands Allows Complementary Apoptotic Function. Mol Cell. 2005;17:393–403. https://doi.org/10.1016/j.molcel.2004.12.030.
15. Núñez-Vázquez S, Sánchez-Vera I, Saura-Esteller J, et al. NOXA upregulation by the prohibitin-binding compound fluorizoline is transcriptionally regulated by integrated stress response-induced ATF3 and ATF4. FEBS J. 2021;288:1271–85. https://doi.org/10.1111/febs.15480.
16. Shi J, Ding F, Dai D, et al. Noxa inhibits oncogenesis through ZNF519 in gastric cancer and is suppressed by hsa-miR-200b-3p. Sci Rep. 2024;14:6568. https://doi.org/10.1038/s41598-024-57099-7.
17. Shang F, Xu L, Liu H, et al. PMAIP1 Enhances DNA Damage and Induces ROS-Mediated Mitochondrial Dysfunction to Suppress Tumorigenesis in Triple-Negative Breast Cancer. Breast J. 2025;2025:7056712. https://doi.org/10.1155/tbj/7056712.
18. Wang H, Zhang H, Kang P, et al. The Epithelial Cell-Associated Gene PMAIP1 Serves as a Prognostic Biomarker for Lung Adenocarcinoma and Can Regulate the Stemness of Lung Cancer. Stem Cells

Int. 2025;2025:2896484. https://doi.org/10.1155/sci/2896484.

19. Li X, Cai Z, Ding S, et al. Integrated single-cell and machine learning analysis identifies PMAIP1 as a novel biomarker for predicting prognosis and immunotherapy response in colorectal cancer. Sci Rep. 2025;16:3685. https://doi.org/10.1038/s41598-025-32933-8.
20. Wang H, Shang F, Wang Y, et al. PMAIP1 regulates the progression of follicular thyroid carcinoma through the Wnt3/FOSL1 pathway. Front Oncol. 2025;15:1502391. https://doi.org/10.3389/fonc.2025.1502391.
21. Pu W, Shi X, Yu P, et al. Single-cell transcriptomic analysis of the tumor ecosystems underlying initiation and progression of papillary thyroid carcinoma. Nat Commun. 2021;12:6058. https://doi.org/10.1038/s41467-021-26343-3.
22. Stuart T, Butler A, Hoffman P, et al. Comprehensive Integration of Single-Cell Data. Cell. 2019;177:1888–902. https://doi.org/10.1016/j.cell.2019.05.031. e21.
23. Lu D-N, Zhang W-C, Lin Y-Z, et al. Single-cell and bulk RNA sequencing reveal heterogeneity and diagnostic markers in papillary thyroid carcinoma lymph-node metastasis. J Endocrinol Invest. 2023;47:1513–30. https://doi.org/10.1007/s40618-023-02262-6.
24. Mallick DJ, Eastman A. AT101 [(-)-Gossypol] Selectively Inhibits MCL1 and Sensitizes Carcinoma to BH3 Mimetics by Inducing and Stabilizing NOXA. Cancers. 2020;12:2298. https://doi.org/10.3390/cancers12082298.
25. Zhang X, Peng W, Fan J, et al. Regulatory role of Chitinase 3-like 1 gene in papillary thyroid carcinoma proved by integration analyses of single-cell sequencing with cohort and experimental validations. Cancer Cell Int. 2023;23:145. https://doi.org/10.1186/s12935-023-02987-7.
26. Gao R, Bai S, Henderson YC, et al. Delineating copy number and clonal substructure in human tumors from single-cell transcriptomes. Nat Biotechnol. 2021;39:599–608. https://doi.org/10.1038/s41587-020-00795-2.
27. Bathe OF, Stretch C. Prognostic Biomarkers for Papillary Thyroid Cancer: Reducing Overtreatment, Improving Clinical Efficiency, and Enhancing Patient Experience. Technol Cancer Res Treat. 2025;24:15330338251361633. https://doi.org/10.1177/15330338251361633.
28. Axten JM, Medina JR, Feng Y, et al. Discovery of 7-Methyl-5-(1-{[3-(trifluoromethyl)phenyl]acetyl}-2,3-dihydro-1 *H* -indol-5-yl)-7 *H* -pyrrolo[2,3- *d*]pyrimidin-4-amine (GSK2606414), a Potent and Selective First-in-Class Inhibitor of Protein Kinase R (PKR)-like Endoplasmic Reticulum Kinase (PERK). J Med Chem. 2012;55:7193–207. https://doi.org/10.1021/jm300713s.
29. Atkins C, Liu Q, Minthorn E, et al. Characterization of a Novel PERK Kinase Inhibitor with Antitumor and Antiangiogenic Activity. Cancer Res. 2013;73:1993–2002. https://doi.org/10.1158/0008-5472.CAN-12-3109.
30. Landa I, Ibrahimpasic T, Boucai L, et al. Genomic and transcriptomic hallmarks of poorly differentiated and anaplastic thyroid cancers. J Clin Invest. 2016;126:1052–66. https://doi.org/10.1172/JCI85271.

31. Molinaro E, Romei C, Biagini A, et al. Anaplastic thyroid carcinoma: from clinicopathology to genetics and advanced therapies. Nat Rev Endocrinol. 2017;13:644–60. https://doi.org/10.1038/nrendo.2017.76.
32. Yang W, Xu X, Xu M, et al. XBP1s Acts as a Tumor Suppressor to Inhibit the EMT Process and Metastasis of Papillary Thyroid Cancer. OTT Volume. 2021;14:2339–48. https://doi.org/10.2147/OTT.S297046.
33. Bi M, Naczki C, Koritzinsky M, et al. ER stress-regulated translation increases tolerance to extreme hypoxia and promotes tumor growth. EMBO J. 2005;24:3470–81. https://doi.org/10.1038/sj.emboj.7600777.
34. Rouschop KMA, Van Den Beucken T, Dubois L, et al. The unfolded protein response protects human tumor cells during hypoxia through regulation of the autophagy genes MAP1LC3B and ATG5. J Clin Invest. 2010;120:127–41. https://doi.org/10.1172/JCI40027.

Figures

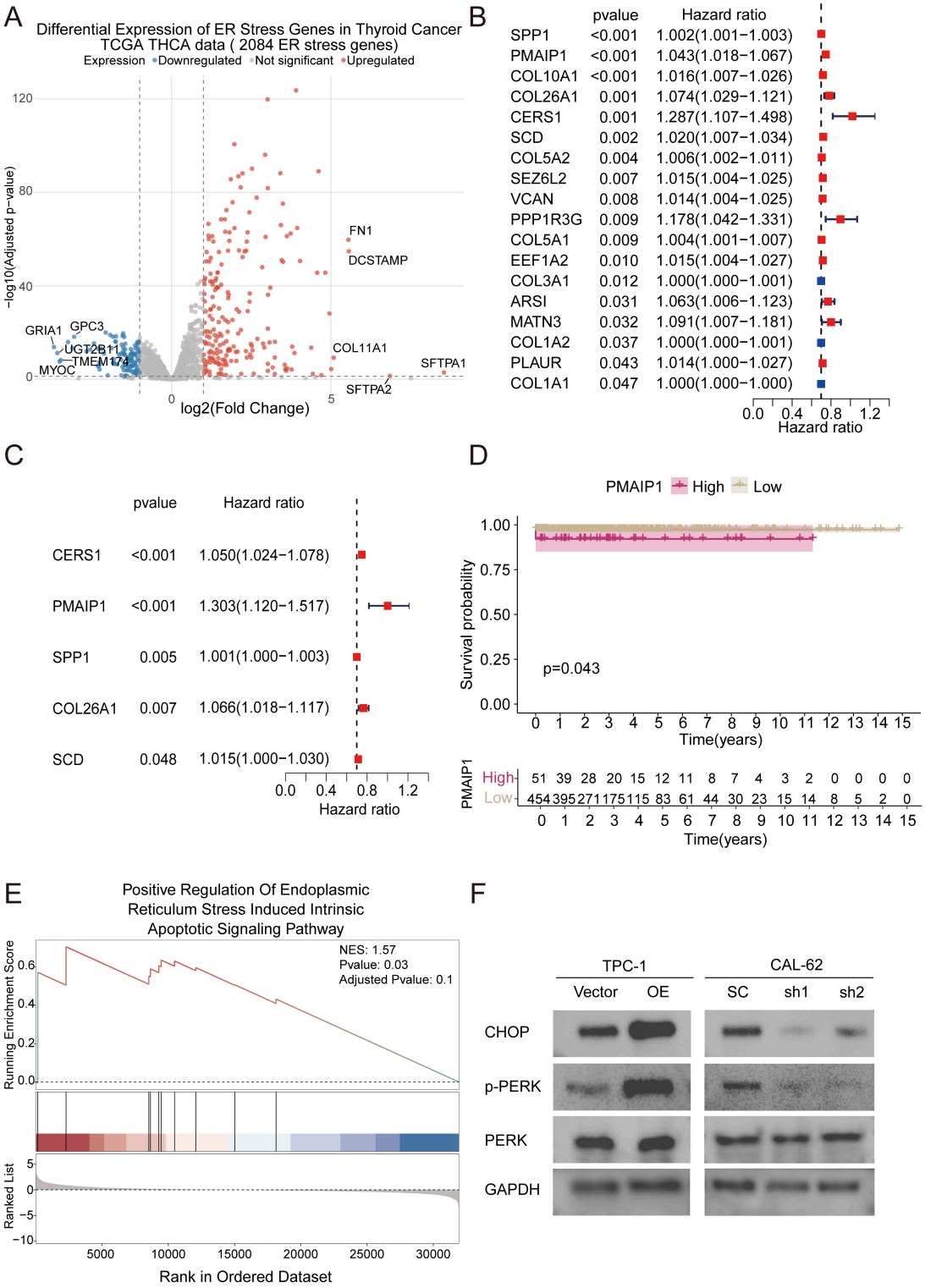


Figure 1

Identification of PMAIP1 as an endoplasmic reticulum stress-related gene associated with poor prognosis in papillary thyroid carcinoma.

(A) Volcano plot showing differential expression of 2,084 endoplasmic reticulum (ER) stress-related genes between papillary thyroid carcinoma (PTC) tissues and adjacent normal tissues in the TCGA-THCA cohort. Differentially expressed genes were identified using $|\log_2 FC|>1$ and FDR<0.05. Red and

blue dots indicate significantly upregulated and downregulated genes, respectively, and gray dots indicate genes without significant differential expression
(B) Forest plot of univariate Cox proportional hazards regression analysis for overall survival (OS), showing ER stress-related genes significantly associated with prognosis
(C) Forest plot of multivariate Cox regression analysis of candidate prognostic genes. PMAIP1 showed the highest hazard ratio among the genes included in the model
(D) Kaplan–Meier analysis of OS in patients stratified according to high or low PMAIP1 expression. The difference between groups was evaluated using the log-rank test
(E) Gene set enrichment analysis (GSEA) showing enrichment of the ER stress-induced apoptotic signaling pathway in tumors with high PMAIP1 expression
(F) Western blot analysis of CHOP, phosphorylated PERK (p-PERK), and total PERK in TPC-1 cells with PMAIP1 overexpression and CAL-62 cells with PMAIP1 knockdown. GAPDH was used as the loading control. OE, PMAIP1 overexpression; sh1 and sh2, PMAIP1-targeting shRNAs; SC, shRNA control

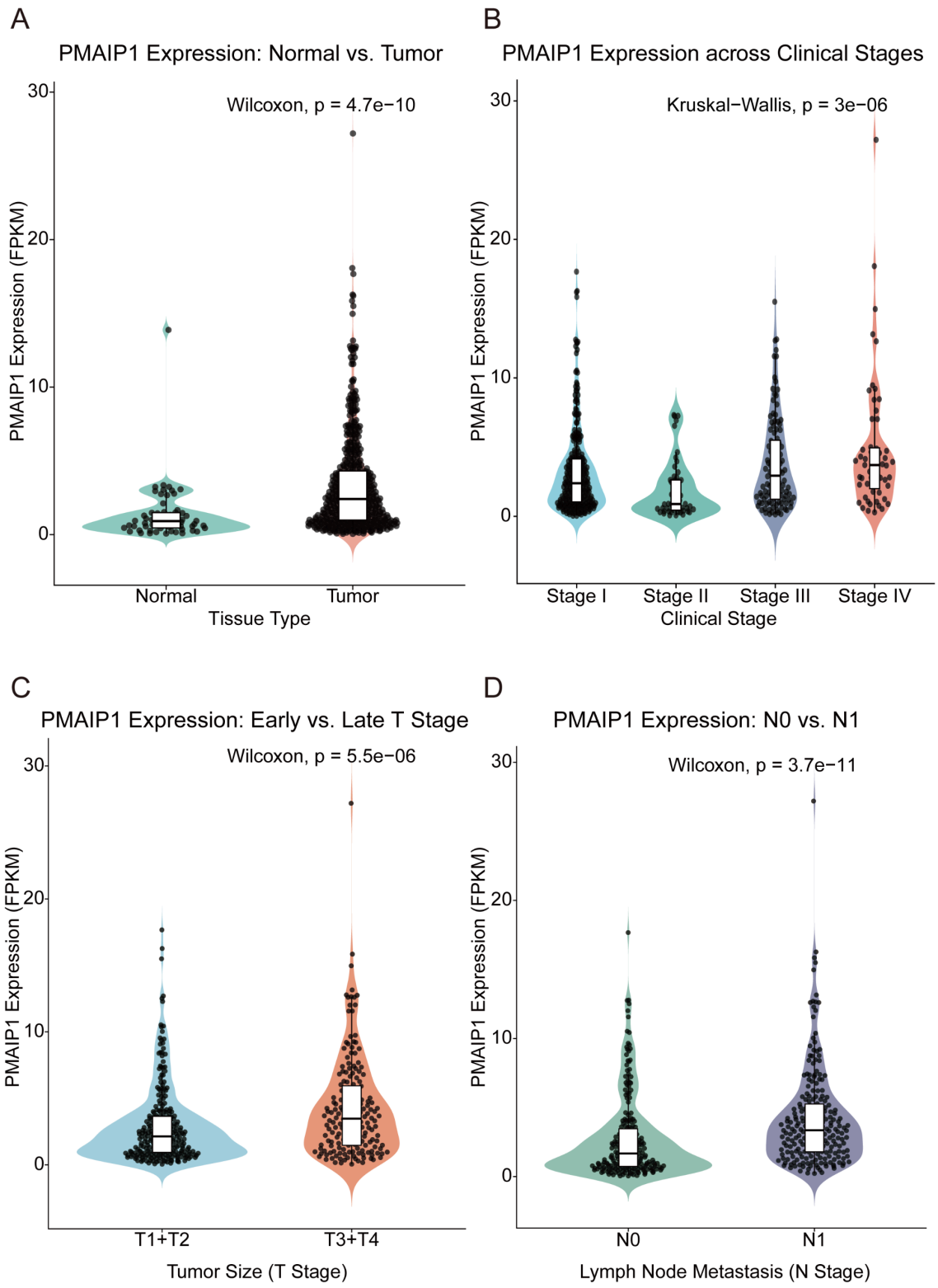


Figure 2

Association between PMAIP1 expression and clinicopathological progression of papillary thyroid carcinoma.

(A) Comparison of PMAIP1 expression between adjacent normal tissues and PTC tissues in the TCGA-THCA cohort (Wilcoxon test, $P=4.7\times10^{-10}$)

(B) PMAIP1 expression across clinical stages I–IV (Kruskal–Wallis test, $P=3.0\times10^{-6}$)

(C) Comparison of PMAIP1 expression between early T-stage (T1–T2) and advanced T-stage (T3–T4) tumors (Wilcoxon test, $P=5.5\times10^{-6}$)

(D) Comparison of PMAIP1 expression between patients without lymph node metastasis (N0) and those with lymph node metastasis (N1) (Wilcoxon test, $P=3.7\times10^{-11}$). PMAIP1 expression is shown as FPKM values

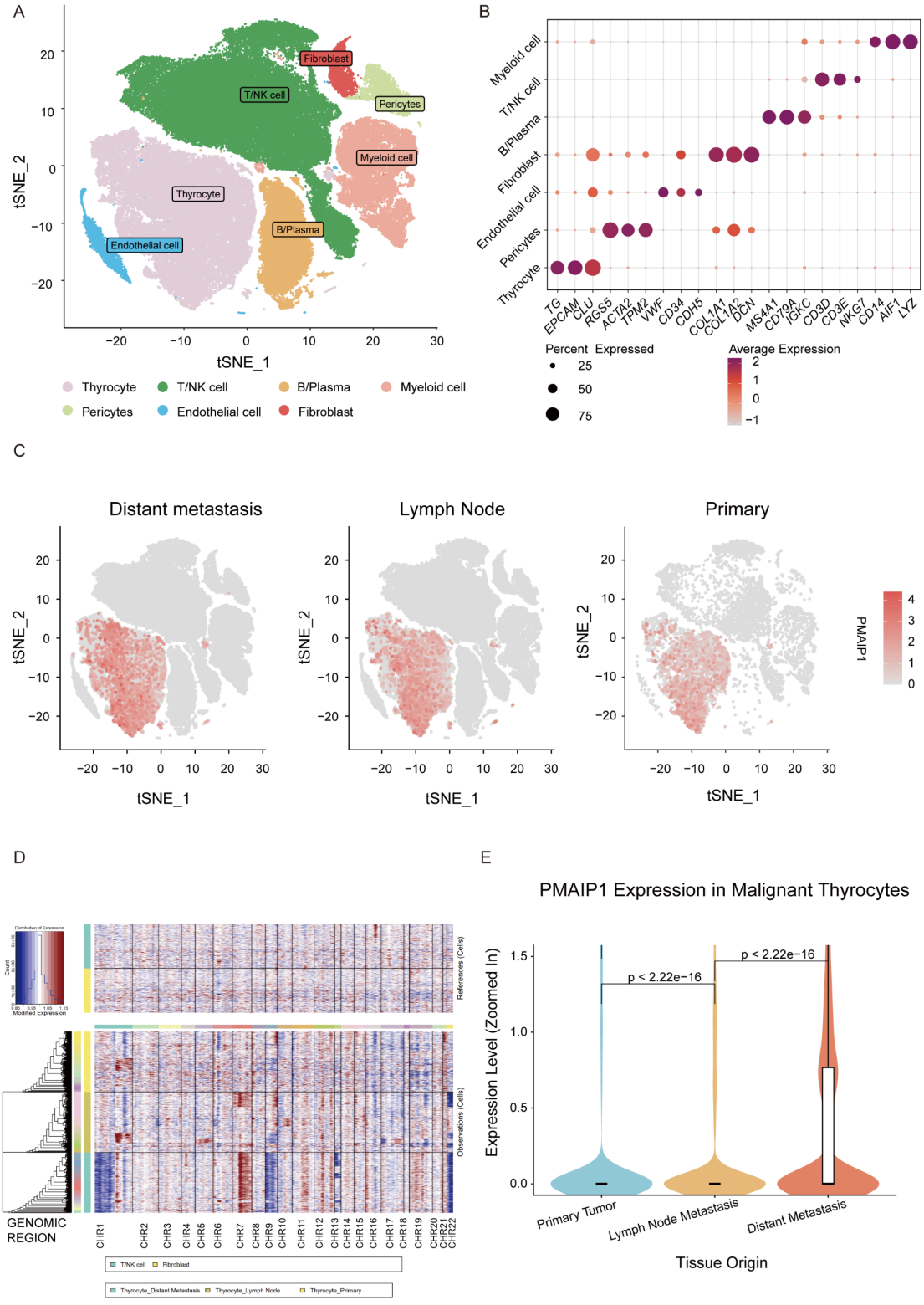


Figure 3

Single-cell transcriptomic analysis reveals enrichment of PMAIP1 in malignant thyrocytes during metastatic progression.
(A) t-distributed stochastic neighbor embedding (t-SNE) visualization of 124,030 cells from the GSE184362 single-cell RNA-sequencing dataset, identifying seven major cell populations: thyrocytes, T/NK cells, B/plasma cells, myeloid cells, fibroblasts, endothelial cells, and pericytes
(B) Dot plot showing the expression of canonical marker genes used for cell-type annotation. Dot size represents the percentage of cells expressing each gene, and color intensity represents average expression
(C) t-SNE feature plots showing the distribution of PMAIP1 expression in primary tumors, lymph node metastases, and distant metastatic lesions
(D) inferCNV analysis of thyroid epithelial cells using T/NK cells and fibroblasts as reference populations, showing large-scale copy-number alterations across thyrocytes derived from primary tumors, lymph node metastases, and distant metastases. Malignant thyrocytes were identified based on copy-number alteration patterns in combination with CopyKAT analysis
(E) Violin plots showing PMAIP1 expression in malignant thyrocytes from primary tumors, lymph node metastases, and distant metastases. Statistical comparisons are indicated in the figure ($P < 2.22\times10^{-16}$)

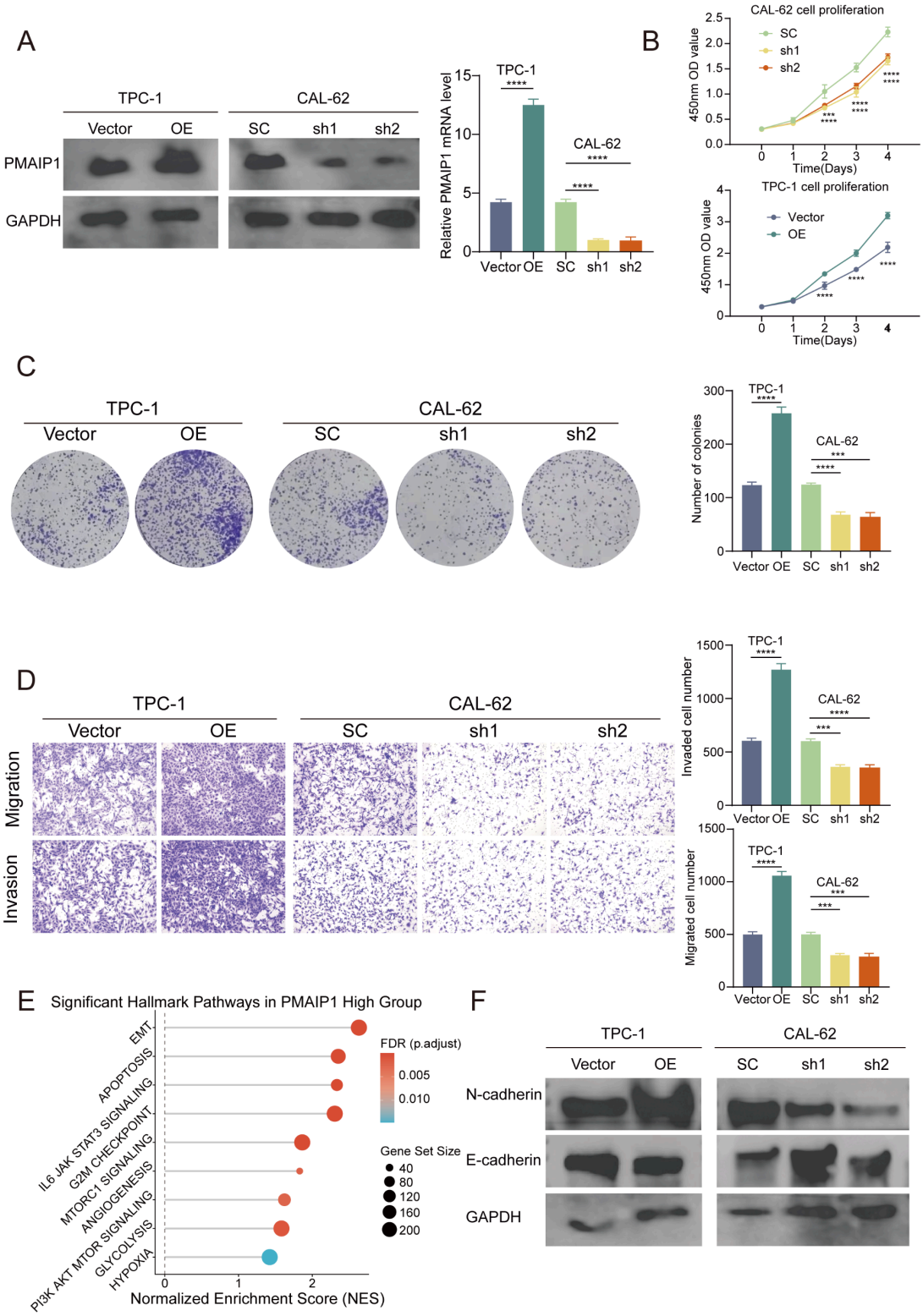


Figure 4

PMAIP1 promotes proliferative, migratory, and invasive phenotypes and is associated with epithelial–mesenchymal transition in thyroid carcinoma cells.

(A) Validation of PMAIP1 overexpression in TPC-1 cells and PMAIP1 knockdown in CAL-62 cells by Western blotting and quantitative real-time PCR (qRT-PCR). GAPDH was used as the loading control for Western blotting

(B) CCK-8 assays evaluating the effects of PMAIP1 overexpression or knockdown on the proliferation of TPC-1 and CAL-62 cells, respectively
(C) Representative images and quantitative analysis of colony formation assays in TPC-1 and CAL-62 cells following PMAIP1 overexpression or knockdown
(D) Representative images and quantitative analysis of Transwell migration and invasion assays showing the effects of PMAIP1 modulation on the migratory and invasive capacities of TPC-1 and CAL-62 cells
(E) GSEA of Hallmark gene sets in the TCGA-THCA cohort showing pathways significantly enriched in the PMAIP1-high group, including epithelial–mesenchymal transition (EMT), apoptosis, IL-6/JAK/STAT3 signaling, G2M checkpoint, mTORC1 signaling, angiogenesis, PI3K/AKT/mTOR signaling, glycolysis, and hypoxia. Dot size represents gene-set size, and color represents the adjusted false discovery rate (FDR); all pathways shown were enriched at FDR < 0.05.
(F) Western blot analysis of the EMT markers N-cadherin and E-cadherin following PMAIP1 overexpression in TPC-1 cells or PMAIP1 knockdown in CAL-62 cells. GAPDH was used as the loading control. OE, PMAIP1 overexpression; sh1 and sh2, PMAIP1-targeting shRNAs; SC, shRNA control

Supplementary Files

This is a list of supplementary files associated with this preprint. Click to download.

- SupplementaryData1.csv
- SupplementaryInformationOriginaluncroppedblots.pdf